References and Notes

1. J. S. Flier, *Proc. Natl. Acad. Sci. U.S.A.* **94**, 4242 (1997); N. Levin, C. Nelson, A. Gurney, R. Vandlen, F. de Sauvage, *ibid.* **93**, 1726 (1996); M. A. Pelleymounter *et al.*, *Science* **269**, 540 (1995); J. L. Halaas *et al.*, *ibid.*, p. 543; L. A. Campfield, F. J. Smith, Y. Guisez, R. Devos, P. Burn, *ibid.*, p. 546.
2. M. Shimabukuro *et al.*, *Proc. Natl. Acad. Sci. U.S.A.* **94**, 4637 (1997); T. Gainsford *et al.*, *ibid.* **93**, 14564 (1996); T. J. Kieffer, R. S. Heller, C. A. Leech, G. G. Holz, J. F. Habener, *Diabetes* **46**, 1087 (1997); R. J. Zachow and D. A. Magoffin, *Endocrinology* **138**, 847 (1997); J. A. Tuominen, P. Ebeling, M. L. Heiman, T. Stephens, V. A. Koivisto, *Acta Physiol. Scand.* **160**, 83 (1997).
3. J. G. Mercer *et al.*, *FEBS Lett.* **387**, 113 (1996); C. Vaisse *et al.*, *Nature Genet.* **14**, 95 (1996).
4. G. H. Lee *et al.*, *Nature* **379**, 632 (1996).
5. D. W. White and L. A. Tartaglia, *Cytokine Growth Factor Rev.* **7**, 303 (1996).
6. H. Baumann *et al.*, *Proc. Natl. Acad. Sci. U.S.A.* **93**, 8374 (1996); N. Ghilardi *et al.*, *ibid.*, p. 6231; C. Bjøbæk *et al.*, *J. Biol. Chem.* **272**, 32686 (1997).
7. R. C. Frederich *et al.*, *J. Clin. Invest.* **96**, 1658 (1995).
8. D. L. Crandall, G. J. Hausman, J. G. Kral, *Microcirculation* **4**, 211 (1997).
9. Peptides based on the sequence of the human leptin receptor (*4*) corresponding to regions within the intracellular or the extracellular domain were synthesized and coupled to keyhole limpet hemocyanin (KLH). The intracellular region peptides were (i) IC-1, for residues 1148 to 1165 at the COOH-terminal end of the receptor (CSTQTHKIMENKMCDLTV), and (ii) IC-2, for residues 1062 to 1078 (KLEGNFPEENNDKKSIY) (*24*). The extracellular region peptides were (i) EC-1, for residues 247 to 263 (ITDDGNLKISWSSPPLV), (ii) EC-2, for residues 473 to 487 (CSDIPSIHPISEPKD), and (iii) EC-3, for residues 753 to 767 (CVIVSWILSPSDYKL) (*24*). The KLH-peptide conjugates were used to generate polyclonal antibodies in rabbits and immunoglobulin (IgG) fractions prepared from bleeds with the highest enzyme-linked immunosorbent assay titers. Unless otherwise indicated, antibodies to IC-1 and IC-2 were combined in equal amounts, producing OB-R_{int} antibodies to intracellular epitopes of the leptin receptor's OB-Rb form. Likewise, equal amounts of antibodies to EC-1, EC-2, and EC-3 were mixed, producing OB-R_{ext} antibodies to extracellular epitopes of the leptin receptor.
10. M. R. Sierra-Honigmann *et al.*, data not shown.
11. Tissue specimens of human abdominal skin and subcutaneous fat were collected during cosmetic surgery. Subcutaneous adipose tissue specimens were also obtained from adult, female, leptin receptor–deficient *db/db* mice or normal *db/+* littermates. After delipidation, the tissue was flash-frozen and cut into 5-μm-thick sections. Sections were stained with anti–OB-R_{int}, *Ulex europaeus* agglutinin I, or normal rabbit serum. After incubation with primary antibodies, tissue sections were developed with secondary horseradish peroxidase–conjugated goat antibody to rabbit IgG with a Vectastain Elite ABC kit (Vector Labs). The slides were counterstained with hematoxylin.
12. Freshly isolated HUVECs (subculture 1) were treated as indicated in Fig. 2A and washed with tris-buffered saline and homogenized on ice with radioimmunoprecipitation assay (RIPA) buffer supplemented with protease inhibitors, and insoluble material was collected by centrifugation at 12,000*g* for 10 min at 4°C. Equal amounts of protein were precleared by incubation with Affi-gel-15 (Bio-Rad) beads for 2 hours at 4°C, and the resin was removed by centrifugation. Lysates were incubated for 6 hours at 4°C with 40 μl of leptin-Affigel beads [containing 30 μg of covalently coupled human recombinant leptin per milliliter of packed Affigel-15 resin; coupling was conducted following the manufacturer's instructions (Bio-Rad)]. Adsorbed complexes were washed with RIPA buffer and boiled with SDS–polyacrylamide gel electrophoresis (SDS-PAGE) sample buffer for 10 min. Proteins were separated by SDS-PAGE with 4 to 20% gradient gels, followed by overnight transfer to nitrocellulose membranes. Immunoblots were developed with anti–OB-R_{int} (*9*) or with RC20 recombinant anti-phosphotyrosine (Transduction Laboratories, Lexington, KY).
13. Confluent monolayers of HUVECs grown in T75 flasks were washed with PBS twice, and total cell extracts were prepared by adding 1 ml of SDS-PAGE sample buffer supplemented with 100 μM dithiothreitol (DTT). Lysed cells were briefly sonicated, and insoluble material was removed by centrifugation. Supernates were collected, boiled for 3 min, and applied to a 4 to 20% gradient gel. Gels were processed for immunoblotting as described (*25*). The PhosphoPlus Stat3 (Tyr^{705}) Antibody kit (New England Biolabs), containing a phospho-specific Stat3 (Tyr^{705}) rabbit polyclonal antibody, was used for detecting the presence of Stat3 and phospho-Stat3 in the cell lysates.
14. HUVECs were washed with PBS, pelleted, and resuspended into a minimal volume of low-salt buffer [20 mM Hepes (pH 7.9), 25% glycerol, 1.5 mM $MgCl_2$, 20 mM KCl, 0.2 mM EDTA, 0.5 mM DTT, 0.2 mM phenylmethylsulfonyl fluoride, and a mixture of protease inhibitors]. After a 15-min incubation on ice, cells were homogenized, and nuclei were collected by centrifugation. The pellet was resuspended in low-salt buffer adjusted to 0.5 M KCl, extracted for 30 min at 4°C, and centrifuged at 25,000*g* for 30 min. Supernates were collected, dialyzed against buffer made 0.1 M with KCl, and divided into small portions kept at −80°C until used.
15. The double-stranded oligonucleotide Stat3 (Santa Cruz Biotechnology, Santa Cruz, CA), was first end-labeled with T4 polynucleotide kinase and [γ-^{32}P]-adenosine triphosphate. After labeling, 10 μg of nuclear extract was incubated with 100,000 cpm (<1 pmol) of ^{32}P-labeled probe for 20 min at room temperature in binding buffer [20 mM tris-HCl (pH 7.9), 50 mM NaCl, 1 mM EDTA, 10% glycerol, 0.1% NP-40, 1 mM DTT, bovine serum albumin (50 μg/ml), and polydeoxyinosine/polydeoxycytosine (2 μg/ml)]. Electrophoresis sample buffer was added to each sample before separation in a nondenaturing gel (89 mM tris, 89 mM boric acid, 10 mM EDTA, and 4.95% acrylamide). Gels were dried and exposed to autoradiography.
16. G. García-Cardeña, P. Oh, J. Liu, J. E. Schnitzer, W. C. Sessa, *Proc. Natl. Acad. Sci. U.S.A.* **93**, 6448 (1996); V. Kundra, B. Anand-Apte, L. A. Feig, B. R. Zetter, *J. Cell Biol.* **130**, 725 (1995).
17. N. Ferrara and W. J. Henzel, *Biochem. Biophys. Res. Commun.* **161**, 851 (1989).
18. R. K. Jain, K. Schlenger, M. Hockel, F. Yuan, *Nature Med.* **3**, 1203 (1997); R. Auerbach, W. Auerbach, I. Polakowski, *Pharmacol. Ther.* **51**, 1 (1991).
19. 3D cultures of HUVECs were established in gel matrices with rat tail Type I collagen at a final concentration of 1.75 mg/ml. The collagen solution was prepared in M199 culture medium and adjusted to fibronectin (90 mg/ml), 150 mM Hepes, and sodium bicarbonate, neutralizing the pH by the addition of 1 M NaOH. HUVECs were added immediately to a final concentration of 2×10^6 cells/ml. Drops (0.2 ml each) of the cell-collagen mixture were added to Petri dishes and placed in a humidified CO_2 incubator at 37°C for 2 to 5 min, allowing them to solidify. Growth medium supplemented with endothelial cell growth supplement with or without human recombinant leptin was then added to each dish. Leptin was replenished every 24 hours. HUVECs were allowed to form tubelike structures for 2 days in culture and were then frozen and sectioned to a thickness of 40 μm. For immunofluorescence analysis, the sections were fixed with acetone (−20°C) and stained with tetramethylrhodamine isothiocyanate–labeled *Ulex europaeus* agglutinin I (0.5 μg/ml) and 4′,6′-diamidino-2-phenylindole (DAPI) (0.0001%).
20. V. P. Castle, V. M. Dixit, P. J. Polverini, *Lab. Invest.* **77**, 51 (1997).
21. K. Koyama *et al.*, *Diabetes* **48**, 1276 (1997).
22. Y. T. Zhou *et al.*, *Proc. Natl. Acad. Sci. U.S.A.* **94**, 6386 (1997).
23. U. Sarmiento *et al.*, *Lab. Invest.* **77**, 243 (1997).
24. Abbreviations for the amino acid residues are as follows: C, Cys; D, Asp; E, Glu; F, Phe; G, Gly; H, His; I, Ile; K, Lys; L, Leu; M, Met; N, Asn; P, Pro; Q, Gln; S, Ser; T, Thr; V, Val; W, Trp; and Y, Tyr.
25. M. R. Sierra-Honigmann, J. R. Bradley, J. S. Pober, *Lab. Invest.* **74**, 684 (1996).

26. We thank T. Buckholz and J. Kupcho for the synthetic peptides and conjugates, L. Friedman for the anti–leptin receptor, L. Benson and G. Davis for HUVEC cultures, D. O'Connor for help in migration studies, and J. Pober for laboratory resources.

5 March 1998; accepted 23 July 1998

Disruption of a Neuropeptide Gene, *flp-1*, Causes Multiple Behavioral Defects in *Caenorhabditis elegans*

Laura S. Nelson,* Marc L. Rosoff,† Chris Li‡

Neuropeptides serve as important signaling molecules in the nervous system. The FMRFamide (Phe-Met-Arg-Phe-amide)–related neuropeptide gene family in the nematode *Caenorhabditis elegans* is composed of at least 18 genes that may encode 53 distinct FMRFamide-related peptides. Disruption of one of these genes, *flp-1*, causes numerous behavioral defects, including uncoordination, hyperactivity, and insensitivity to high osmolarity. Conversely, overexpression of *flp-1* results in the reciprocal phenotypes. On the basis of epistasis analysis, *flp-1* gene products appear to signal upstream of a G protein–coupled second messenger system. These results demonstrate that varying the levels of FLP-1 neuropeptides can profoundly affect behavior and that members of this large neuropeptide gene family are not functionally redundant in *C. elegans*.

FMRFamide-related neuropeptides (FaRPs) represent a large family of peptides that have been implicated as neurotransmitters or neuromodulators in many invertebrate and vertebrate behaviors, including muscular control (*1*), cardioregulation (*2*), pain modulation (*3*),

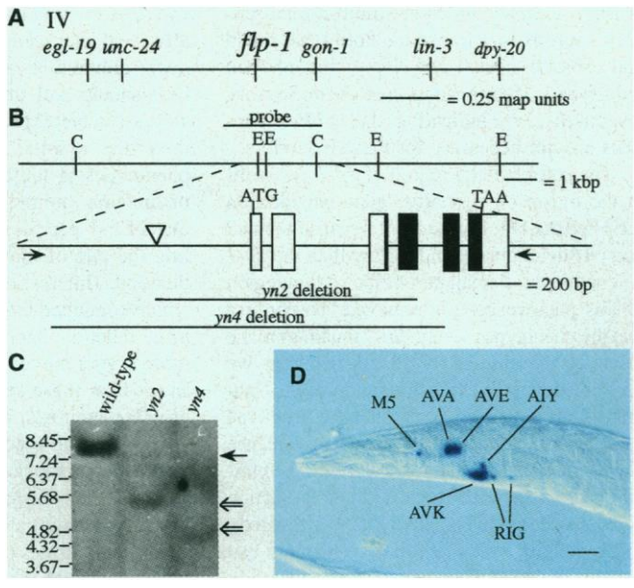

Fig. 1. *flp-1* deletion alleles. (**A**) Genetic position of *flp-1* on the right arm of chromosome IV. (**B**) Genomic organization of *flp-1*. Top line: partial restriction map of the *flp-1* genomic region. E, Eco RI; C, Cla I. Bottom line: Expanded genomic region to show organization of *flp-1*. Exons are indicated as boxes (peptide coding sequences are indicated in black), introns as lines; the site of the Tc1 insertion is indicated by an inverted triangle. Two deletions of the *flp-1* gene were isolated by PCR screening of populations of Tc1 insertion strains for an imprecise Tc1 excision (*13*). The extent of the *yn2* (1.4 kbp) and *yn4* (2.1 kbp) deletions are shown; both deletions remove upstream and coding regions. Primers used to screen for deletions are indicated by arrows. (**C**) Backcrossed *yn2* and *yn4* strains are homozygous deletion lines. Genomic DNA was isolated from backcrossed *yn2* and *yn4* animals, digested with Cla I, and Southern blotted. The position of the probe is shown in (B). Solid arrow indicates wild-type hybridizing fragment; double arrows indicate smaller hybridizing fragments resulting from the *yn2* and *yn4* deletions. No hybridizing fragment corresponding to the wild-type fragment is detected in DNA from homozygous *yn2* and *yn4* animals. Molecular weight markers (kilobase pairs) are indicated to the left. (**D**) Expression of *flp-1* in wild-type animals is detected only in anterior head neurons. Transgenic animals were stained for β-galactosidase activity to visualize expression of *flp-1-lacZ* reporter constructs (*10*). Scale bar, 25 μm.

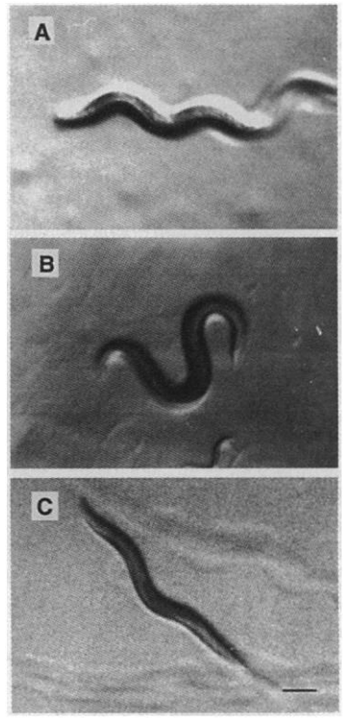

Fig. 2. Varying the level of *flp-1* expression has reciprocal effects on locomotion. (**A**) Wild-type animal shows a characteristic sinusoidal waveform; sinusoidal tracks can also be seen in the bacterial lawn. (**B**) *flp-1(yn2)* animal. *flp-1(yn2)* animals show an exaggerated waveform characterized by an increased wave amplitude. *flp-1(yn4)* animals had a less loopy phenotype than *flp-1(yn2)* animals (Table 1). (**C**) Animal in which *flp-1* is overexpressed (*ynIs9*). After heat shock, transgenic animals carrying a *flp-1* cDNA under the control of a heat shock promoter show a much flattened waveform compared to that of wild-type animals (Table 1). Scale bar, 0.1 mm.

and learning (*4*). Although a single organism may express multiple FaRPs encoded by multiple genes (*5*), little is known about the function of distinct FaRPs or the cellular and molecular mechanisms whereby different FaRPs exert their effects. We used a genetic approach to determine the role of a distinct set of FaRPs in the simple nematode model system, *Caenorhabditis elegans*.

Eighteen genes, designated *flp-1* (FMRFamide-like peptide) through *flp-18*, in *C. elegans* potentially encode 53 distinct FaRPs, all of which contain the COOH-terminal RFamide (Arg-Phe-NH_2) epitope characteristic of the FaRP family. At least 15 of these *flp* genes are expressed (*6, 7*). The *flp-1* gene consists of six exons and produces two transcripts by alternative splicing; these two transcripts encode seven distinct FaRPs, which range from seven to ten amino acids in length and which contain a FLRFamide sequence at their COOH-termini (*6*). By standard two- and three-factor crosses, we determined that *flp-1* is located on the right arm of chromosome IV between *unc-24* and *dpy-20* (Fig. 1A) (*8*). This map position has been confirmed by the *C. elegans* Genome Sequencing Consortium (*9*), which places *flp-1* on cosmid F23B2. To determine the expression pattern of *flp-1*, transgenic animals carrying *lacZ* or green fluorescent protein (GFP) reporter constructs were generated. Thus far, we have detected *flp-1* expression only in neurons in the anterior region of the animal (Fig. 1D) (*10*). *flp-1*–expressing cells include AVK, AVA, AVE, RIG, RMG, AIY, AIA, and M5. These cells are a subset of the FMRFamide-like immunoreactive cells previously described (*11*).

To determine the function of *flp-1* in *C. elegans*, we screened for *flp-1* deletion mutants by using a Tc1 transposon-dependent polymerase chain reaction (PCR) method (*12*). Populations of a Tc1 transposon insertional allele of *flp-1* [NL242 (*pk41*)] were screened for germline deletions (*13*). Mutants with 1.4 kilobase pairs (kbp) [NY7 (*yn2*)] and 2.1 kbp [NY16 (*yn4*)] deleted from the *flp-1* gene were isolated (Fig. 1B). By DNA sequence analysis, we determined that the *yn2* deletion removed 570 bp of the promoter sequence, the start site of transcription (*6*), exons 1 through 3, and most of exon 4; the *yn4* deletion removed 1.1 kbp of the promoter sequence, the start site of transcription, and exons 1 through 4. Thus, both alleles are likely to represent severe loss of *flp-1* function. DNA was isolated for Southern blot analysis to confirm the presence of the deletions in homozygous strains (Fig. 1C) (*14*). The pattern of FMRFamide-like immunoreactivity did not differ between *flp-1* mutants and wild-type animals (*15*), suggesting that individual cells expressing FLP-1 peptides also express other FaRPs.

To determine how loss of FLP-1 peptides might affect behavior, both *flp-1* mutant strains were backcrossed multiple times into a wild-type Bristol background to remove unlinked copies of Tc1. Several motor defects were immediately apparent in *flp-1* animals. Wild-type animals move on a food source with a characteristic sinusoidal waveform (*16*). By contrast, homozygous *flp-1* mutants had loopy, uncoordinated movement; the sinusoidal waveform was exaggerated (Fig. 2), such that the wave amplitude was significantly greater than that of the wild type (Table 1). The action of FLP-1 peptides on waveform may be through the *flp-1*–expressing interneurons, AVE and AVA, both of which synapse onto ventral nerve cord

Department of Biology, Boston University, 5 Cummington Street, Boston, MA 02215, USA.

*Present address: Axys Pharmaceuticals, 180 Kimball Way, South San Francisco, CA 94080, USA.
†Present address: Elan Pharmaceuticals, 3760 Haven Avenue, Menlo Park, CA 94025, USA.
‡To whom correspondence should be addressed. E-mail: li@bu.edu

motoneurons important for coordinated movement in the animal (*17*).

A second obvious motor abnormality seen in *flp-1* animals was hyperactivity, characterized by an increased rate of movement and a tendency to crawl off the agar onto the side of the plate even in the presence of food (wandering). To quantitate hyperactivity, we counted the number of body bends per minute on a food source and recorded the frequency with which the animals crawled off the agar. Homozygous *yn2* animals were significantly more hyperactive than wild-type animals and showed significant wandering behavior (Table 1). Surprisingly, homozygous *yn4* animals, which have the larger deletion in *flp-1*, were not as hyperactive as *yn2* animals and showed little wandering behavior (Table 1). This difference in behavior between the two strains suggests that there is a low level of expression from the remaining *flp-1* exons in *yn4* animals, perhaps due to expression from a cryptic promoter, as has been reported for other *C. elegans* genes with deletions in the 5′ region (*18*). Alternatively, a novel deleterious product may be made in *yn2* animals, resulting in a more severe phenotype. Transheterozygotes with one *yn2* and one *yn4* allele, however, show phenotypes (hyperactivity, wandering, and uncoordination) similar to *yn4* homozygotes (*15*), suggesting that the more severe phenotypes in the *yn2* animals are not due to a novel product. Hyperactive and wandering behaviors are also seen in food-deprived animals (*19*). Because *flp-1* animals have normal chemotaxis responses to soluble and volatile substances (including food), *flp-1* animals may be defective in the pathway responsible for signaling animals to slow down once they reach food.

Several sensory behaviors were also examined in the *flp-1* deletion animals. Wild-type animals recoil when lightly touched on the nose (nose touch sensitivity) (*20*), move backward or forward when gently touched on the head or tail, respectively (mechanosensitivity) (*21*), avoid areas of high osmolarity (osmotic avoidance) (*22*), and are attracted or repelled by specific soluble and volatile chemicals (chemosensitivity) (*23*); for the most part, these four behaviors are mediated by independent neural circuits. Two sensory defects were detected in *flp-1* animals (Table 1). First, *flp-1* mutants were nose touch–insensitive: homozygous *flp-1* animals responded to nose touch stimuli less than 30% of the time compared to ~80% of the time for wild-type animals. Second, homozygous *flp-1* animals were defective for osmotic avoidance and did not hesitate to cross a high osmolarity barrier. FLP-1 peptides, therefore, are necessary in the pathways for response to nose touch and high osmolarity. Two *flp-1*–expressing interneurons, AVA and AIA, receive direct synaptic input from the ASH sensory neurons, which are multi-modal sensory neurons that transduce both nose touch and osmotic stimuli (*20*). *flp-1* mutants had wild-type body mechano- and chemosensory responses (*24*), indicating that FLP-1 peptides are not necessary for these behaviors.

The entire coding region of *flp-1* lies within the intron of a putative gene encoded on the opposite DNA strand (*9*); because the *yn2* and *yn4* deletions extend further than the *flp-1* coding region, a small part of the coding region of this putative gene is removed. To confirm that the phenotypes seen in *flp-1* mutants are the result of the absence of FLP-1 peptides, we performed germline transformation of *flp-1* animals with a plasmid containing the wild-type *flp-1* gene and 6 kbp of *flp-1* upstream sequence (*25*). *flp-1* transgenic animals carrying the plasmid (n = 37) were rescued for coordination (67% rescued), hyperactivity (70% rescued), and wandering (94% rescued), confirming that control of these behaviors is dependent on FLP-1 peptides.

To determine the effect of overexpression of FLP-1 peptides, we generated transgenic animals carrying a *flp-1* cDNA under the control of a heat shock promoter, *hsp 16-2* (*26, 27*), in a wild-type (*ynIs9* and *ynIs10*) or a *flp-1* (*yn2;ynI*s9) mutant background (*28*). When *ynIs9* or *ynIs10* adult animals were heat-shocked for 1 to 2 hours at 33°C, their movement was decreased and animals showed a flattened waveform compared to that of wild-type animals that had been similarly heat-shocked (Fig. 2 and Table 1). Furthermore, although 80% of wild-type (n = 90) and *flp-1* (n = 41) animals continued to move after heat shock, only 32% of the *flp-1* transgenic animals (n = 56) were moving after heat shock, and this movement was highly sluggish. Overexpression of FLP-1 peptides, therefore, results in reciprocal movement phenotypes to those seen in *flp-1* reduction-of-function animals, further demonstrating that FLP-1 peptides are involved in controlling the rate of movement and muscle coordination. Interestingly, *yn2;ynIs9* animals, which contained the heat shock transgene in a *flp-1* deletion background, showed slightly more severe movement phenotypes after heat shock than those seen in heat-shocked *ynIs9* or *ynIs10* animals, which contained the transgene in a wild-type background. The waveform of heat-shocked *yn2;ynIs9* animals disappeared and basically corresponded to the width of the animal (Table 1); moreover, less *yn2;ynIs9* animals (22%; n = 27) were moving after heat shock than *yn9* or *yn10* animals (32%). Recovery from the effects of *flp-1* overexpression occurred after about 18 hours (n = 24). The increased severity of the behaviors in a *flp-1* deletion background may be due to a compensatory up-regulation of the peptide receptors, resulting in greater sensitivity when the peptides are overexpressed. Because of the extreme sluggishness of the transgenic animals after heat shock, we were unable to test the animals for osmotic avoidance. However, *yn2;ynIs9* animals responded to nose-touch when *flp-1* was overexpressed; moreover, this sensitivity was reversible, as the animals became nose touch–insensitive

Table 1. Phenotypes seen in *flp-1* deletion and overexpression animals. Adult hermaphrodites (except where noted) were scored for nose touch, osmotic avoidance, uncoordination, movement rate, and wandering. Mean values ± standard errors are reported. Numbers of animals tested are indicated in parentheses. ND, not determined; NC, not calculated.

Genotype	Nose touch (percent response)†	Osmotic avoidance (escape time in minutes)‡	Uncoordination (wave amplitude in millimeters)§	Movement rate (body bends/min)‖	Wandering (percent off agar after 40 hours)¶
Wild type	79.0 ± 2.9 (n = 21)	20.2 ± 1.5 (n = 50)	0.20 ± 0.01 (A; n = 55) 0.15 ± 0.01 (L4; n = 8)	7.8 ± 0.8 (n = 53)	1.4 ± 0.0 (n = 70)
flp-1(yn2)	14.2 ± 2.6* (n = 12)	4.5 ± 0.5* (n = 40)	0.35 ± 0.01* (A; n = 51)	13.8 ± 1.8* (n = 31)	65.0 ± 0.1* (n = 60)
flp-1(yn4)	29.7 ± 4.0* (n = 16)	3.2 ± 0.4* (n = 25)	0.23 ± 0.01* (L4; n = 8)	10.1 ± 1.7 (n = 22)	15.0 ± 0.6* (n = 40)
flp-1(ynIs9)	ND	ND	0.15 ± 0.00* (A; n = 37)	3.2 ± 1.0 (n = 21)*	ND
flp-1(yn2; ynIs9)	65.9 ± 0.1 (n = 27)	ND	0.10 ± 0.01* (A; n = 7)	NC#	ND

*Significantly different (Neuman-Keuls tests, $P < 0.05$) from the wild type (significance not determined for *yn2;ynIs9* animals in nose-touch assay). †Animals were lightly touched on the nose with an eyebrow hair. Each animal was scored 10 times; the mean response for the animal was considered one trial. ‡Animals were placed in a ring of 6 M glycerol. The time for the animal to cross the ring was measured. §Amplitude was measured as the distance from the peak to the trough of the sine wave. A = adult animals; L4 = animals in the fourth larval stage. ‖The number of body bends an animal made in 1 min was counted. The movement of animals and percent of animals moving at any time is somewhat variable. Animals that did not move during the minute were also included in the calculations (four animals for the wild type, three animals for *yn2*, five animals for *yn4*, and seven animals for *ynIs9*). #Movement rate for *yn2;ynIs9* animals could not be calculated, because most heat-shocked transgenic animals did not move. ¶Animals were individually plated and scored after 40 hours.

again after overnight recovery (Table 1).

Serotonin (5-hydroxytryptamine or 5-HT) also regulates the rate of movement in *C. elegans*. Exogenous 5-HT has an inhibitory effect on movement in *C. elegans* (*29*), whereas 5-HT–deficient animals are hyperactive (*30*). To determine whether FLP-1 peptides and 5-HT are involved in a common pathway controlling movement, we tested whether *flp-1* animals are sensitive to exogenous 5-HT. When exposed to 6.5 mM 5-HT, the movement of wild-type animals was significantly inhibited (Table 2). By contrast, the movement of *flp-1* animals was not significantly decreased by 5-HT (Table 2). FLP-1 peptides, therefore, appear to act downstream or parallel to serotonin in this signaling pathway. For instance, the *flp-1*–expressing interneurons AVA, AVE, or AIA could be influenced by the serotonergic NSM (*29*) to modulate locomotion.

Most FaRPs are likely to signal through a heterotrimeric GTP–binding protein (G protein)–coupled receptor (*31*); to date, however, the only FaRP receptor isolated is a FMRFamide-gated sodium channel (*32*). *Caenorhabditis elegans* animals with a mutation in a G protein subunit, such as $G\alpha_o$ (*goa-1*), $G\alpha_q$ (*egl-30*), or Gβ (*gpb-1*), show multiple phenotypes, including uncoordination and movement rate phenotypes similar to those in *flp-1* mutants (*30, 33*), suggesting that FLP-1 peptides act via a G protein–coupled second messenger system. To test this hypothesis, we generated double mutants between *flp-1* and G protein–subunit mutant animals as follows: a *flp-1* heat shock overexpression animal (*ynIs9*) was mated with a $G\alpha_o$ loss-of-function [*goa-1(n363)*] (*30*) or a $G\alpha_q$ gain-of-function [*egl-30(syEx125)*] mutant animal (*33*), and a *flp-1(yn2)* reduction-of-function mutant animal was mated with a constitutively active $G\alpha_o$ [*goa-1(syIs9)*] (*33*), a loss-of-function $G\alpha_q$ [*egl-30(ad809)*] (*33*), or a Gβ overexpression [*gpb-1(pkIs372)*] (*33*) mutant animal. In each case, the resulting double mutant demonstrated uncoordination and movement rate phenotypes similar to those of the single G protein–subunit mutant (Table 3). These results suggest that FLP-1 peptides signal upstream of these G proteins to control coordinated movement. Recent work has shown that $G\alpha_q$ is likely to act downstream of $G\alpha_o$ (*34*); FLP-1 may be one of the signals that activate the G protein pathway.

Our work demonstrates that individual FaRP-encoding genes have unique functions in an organism. FLP-1 peptides are critical in the functioning of multiple sensory and locomotory pathways and act as neuromodulators of the classical neurotransmitter serotonin in movement inhibition. Varying the levels of FLP-1 peptides results in a spectrum of behavioral phenotypes in *C. elegans*, as demonstrated by the range of phenotypes seen in the reduction-of-function animals, *yn2* and *yn4*, and the *flp-1*-induced overexpression animals. Seven distinct FaRPs are encoded by *flp-1*; it is unknown whether expression of any FLP-1 peptide is sufficient for normal sensory and motor function or whether certain peptides have unique sensory or motor functions. However, FLP-1 peptides have functions distinct from other FaRPs in *C. elegans*. Given the number of additional *flp* genes and the possibility that each gene or peptide has specific, nonredundant functions, the possible complexity of FaRP activity in *C. elegans* is enormous. *Caenorhabditis elegans* will provide a valuable system in which the function of a complex neuropeptide gene family can be elucidated.

Table 2. *flp-1* deletion animals are resistant to serotonin-induced movement inhibition. Adult animals were placed on agar plates with or without 6.5 mM serotonin for 2 hours. Movement rates in the presence (#) or absence (∧) of food (absence of food increases movement rates of animals) were determined as in Table 1.

Genotype	Movement rate (body bends/min)	
	No serotonin	With serotonin
Wild type	7.8 ± 0.8 (n = 53)#	1.5 ± 0.5 (n = 25)#*
	12.0 ± 1.6 (n = 20)∧	0.9 ± 0.2 (n = 14)∧*
flp-1(yn2)	13.8 ± 1.8 (n = 31)#	11.8 ± 2.4 (n = 25)#
flp-1(yn4)	19.1 ± 1.9 (n = 20)∧	15.1 ± 3.7 (n = 14)∧

*Significantly different (Mann-Whitney tests, $P < 0.05$) from the wild type with no serotonin.

Table 3. FLP-1 peptides signal upstream of a G protein–mediated pathway. Double mutants with an *flp-1* allele and an allele of one of the G protein subunits were generated; the phenotype of adult animals was scored as in Table 1.

Genotype	Uncoordination (wave amplitude in millimeters)	Movement rate (body bends/min)
Wild type	0.20 ± 0.01 (n = 55)	7.8 ± 0.8 (n = 53)
flp-1(yn2)	0.35 ± 0.01 (n = 51)	13.1 ± 1.8 (n = 31)
goa-1(syIs9)	0.13 ± 0.01 (n = 18)	1.4 ± 0.4 (n = 10)
flp-1(yn2); goa(syIs9)	0.12 ± 0.00 (n = 20)	0.1 ± 0.1 (n = 12)
egl-30(ad809)	0.16 ± 0.01 (n = 20)	0.3 ± 0.3 (n = 11)
egl-30(ad809); flp-1(yn2)	0.14 ± 0.01 (n = 20)	Not calculated*
gpb-1(pkIs372)	0.13 ± 0.01 (n = 20)	1.3 ± 0.4 (n = 14)
flp-1(yn2); gpb-1(pkIs372)	0.19 ± 0.01 (n = 20)	0.4 ± 0.3 (n = 14)
flp-1(ynIs9)	0.15 ± 0.00 (n = 37)	3.2 ± 1.0 (n = 21)
goa-1(n363)	0.24 ± 0.00 (n = 18)	12.4 ± 1.1 (n = 18)†
flp-1(ynIs9); goa-1(n363)	0.26 ± 0.01 (n = 10)	13.4 ± 2.3 (n = 10)
egl-30(syEx125)	0.24 ± 0.01 (n = 45)	7.6 ± 1.9 (n = 10)†
flp-1(ynIs9); egl-30(syEx125)	0.20 ± 0.01 (n = 20)	7.4 ± 1.6 (n = 15)

*Movement rates could not be calculated because animals did not move (91.8%) or barely moved (8.2%). †Movement rates were calculated 1 hour after heat shock. *egl-30* animals did not fully recover to their pre–heat shock values at this time.

References and Notes

1. For reviews, see R. B. Raffa, *Peptides* **9**, 915 (1988); D. J. A. Brownlee, I. Fairweather, L. Holden-Dye, R. J. Walker, *Parasitol. Today* **12**, 343 (1996); A. G. Maule *et al.*, *ibid.*, p. 351.
2. D. A. Price and M. J. Greenberg, *Science* **197**, 670 (1977); J. Kuhlman, C. Li, R. L. Calabrese, *J. Neurosci.* **5**, 2310 (1985); T. M. Wong, M. J. Greenberg, S. Y. H. Tse, *Comp. Biochem. Physiol. C* **81**, 175 (1985).
3. J. Tang, H.-Y. T. Yang, E. Costa, *Proc. Natl. Acad. Sci. U.S.A.* **81**, 5002 (1984); H.-Y. T. Yang, W. Fratta, E. A. Majane, E. Costa, *ibid.* **82**, 7757 (1985); M. Kavaliers, *Neurosci. Lett.* **115**, 307 (1990).
4. S. L. Mackey *et al.*, *Proc. Natl. Acad. Sci. U.S.A.* **84**, 8730 (1987); S. A. Small, E. R. Kandel, R. D. Hawkins, *Science* **243**, 1603 (1989); M. Kavaliers and D. D. Colwell, *Neurosci. Lett.* **157**, 75 (1993).
5. J. R. Nambu *et al.*, *Neuron* **1**, 55 (1988); R. Nichols, S. A. Schneuwly, J. E. Dixon, *J. Biol. Chem.* **263**, 12167 (1988); L. Schneider and P. H. Taghert, *Proc. Natl. Acad. Sci. U.S.A.* **85**, 1993 (1988); R. Nichols, *J. Mol. Neurosci.* **3**, 213 (1992).
6. M. L. Rosoff, T. R. Bürglin, C. Li, *J. Neurosci.* **12**, 2356 (1992); M. L. Rosoff, K. E. Doble, D. A. Price, C. Li, *Peptides* **14**, 331 (1993).
7. L. S. Nelson, K. Kim, J. E. Memmott, C. Li, *Mol. Brain Res.* **58**, 103 (1998).
8. DNA from a *flp-1*::Tc1 insertion strain, NL242 *(pk41)*, was isolated as described [B. D. Williams, B. Schrank, C. Huynh, R. Shownkeen, R. H. Waterston, *Genetics* **131**, 609 (1992)] and amplified with a *flp-1*–specific and Tc1-specific primer. The Tc1 transposon was inserted 565 bp upstream of the start site of transcription. The Tc1 transposon in the *flp-1*::Tc1 insertional animals *(pk41)* was used as a genotypic marker in two- and three-factor crosses; *flp-1* was positioned to chromosome IV by two-factor crosses. To position *flp-1* more precisely, the double mutant *unc-5* (IV) *dpy-20* (IV) was mated to *pk41*; 19 Dpy-20, non–Unc-5 and 26 Unc-5, non–Dpy-20 recombinants carried the Tc1 marker, while 12 Unc-5, non–Dpy-20 and 24 Dpy-20, non–Unc-5 recombinants did not. These data indicate that *flp-1* is located at approximately +4.0 map units on chromosome IV.
9. J. E. Sulston *et al.*, *Nature* **356**, 37 (1992); R. Wilson *et al.*, *ibid.* **368**, 32 (1994).
10. Varying amounts of the *flp-1* upstream region (107 bp, 232 bp, 332 bp, 1.5 kbp, and 6 kbp) were

subcloned into *lacZ* (pPD21.28 and pPD16.01) or GFP (pPD95.75) reporter constructs (*26*) and assayed for β-galactosidase activity or fluorescence. One translational fusion construct in which 1.5 kbp of the *flp-1* upstream region and part of the coding region was fused in-frame to the *lacZ* gene and the remaining part of the coding region was placed after the stop codon of the *lacZ* gene was also made. Reporter constructs were co-injected with the *rol-6* pRF4 plasmid as described [C. C. Mello, J. M. Kramer, D. Stinchcomb, V. Ambros, *EMBO J.* **10**, 3959 (1991)]. All transgenic lines showed *flp-1* expression only in anterior head neurons, and for the most part, all transgenic lines had the same expression pattern.

11. K. Schinkmann and C. Li, *J. Comp. Neurol.* **315**, 1 (1992).
12. A. Rushforth, B. Saari, P. Anderson, *Mol. Cell. Biol.* **13**, 902 (1993); R. R. Zwaal, A. Broeks, J. van Meurs, J. T. M. Groenen, R. H. A. Plasterk, *Proc. Natl. Acad. Sci. U.S.A.* **90**, 7431 (1993).
13. Populations of *flp-1*::Tc1 *(pk41)* animals were screened as described (*12*). The deletion amplification products were subcloned into the TA cloning vector (Invitrogen) and sequenced using the USB Sequenase 2.0 kit.
14. Southern (DNA) blot analysis was performed as described [J. Sambrook, E. F. Fritsch, T. Maniatis, *Molecular Cloning: A Laboratory Manual* (Cold Spring Harbor Laboratory Press, Cold Spring Harbor, NY, 1989) with a digoxygenin-labeled probe (Boerhinger Mannheim Genius System). Detection was performed with a chemiluminescent substrate (Boehringer Mannheim Genius System).
15. L. S. Nelson, data not shown.
16. S. Brenner, *Genetics* **77**, 71 (1984).
17. J. G. White, E. Southgate, J. N. Thomson, S. Brenner, *Philos. Trans. R. Soc. London Ser. B* **314**, 1 (1986).
18. C. M. Coburn and C. J. Bargmann, *Neuron* **17**, 695 (1996).
19. L. S. Nelson, unpublished observations.
20. J. M. Kaplan and H. R. Horvitz, *Proc. Natl. Acad. Sci. U.S.A.* **90**, 2227 (1993).
21. M. Chalfie and M. Au, *Science* **243**, 1027 (1989).
22. J. G. Culotti and R. L. Russell, *Genetics* **90**, 243 (1978).
23. S. Ward, *Proc. Natl. Acad. Sci. U.S.A.* **70**, 817 (1973); D. B. Dusenbery, *J. Exp. Biol.* **188**, 41 (1974); C. I. Bargmann and H. R. Horvitz, *Neuron* **7**, 729 (1991).
24. L. S. Nelson and C. Li, data not shown.
25. The 6 kbp *flp-1* upstream region was amplified from wild-type genomic DNA and inserted into a construct with the *flp-1* coding region to yield LN/B3-SB. *flp-1(yn2); lin-15(n765ts)* animals were co-injected with LN/B3-SB (50 to 100 μg/ml) and JM24 (*lin-15*; 50 μg/ml). Transgenic animals (selected by rescue of the Lin-15 phenotype at 20°C) were scored for rescue of *flp-1* phenotypes as described.
26. A. Fire, S. White, D. Dixon, *Gene* **93**, 189 (1990).
27. E. G. Stringham, D. K. Dixon, D. Jones, E. P. M. Candido, *Mol. Biol. Cell.* **3**, 221 (1992).
28. A *flp-1* cDNA, 3-3F, was subcloned into the hsp vector pPD49.78 (*26*) to yield HSP-FLP1. *lin-15(n765ts)* animals were co-injected with HSP-FLP1 (100 μg/ml) and JM24 (*lin-15*; 50 μg/ml). Transgenic animals were selected by rescue of the Lin-15 phenotype at 20°C; the transgene was integrated by exposing transgenic animals to cobalt irradiation as described [J. C. Way, L. Wang, J.-Q. Run, A. Wang, *Genes Dev.* **5**, 2199 (1991)]. Two integrated lines (*ynIs9* and *ynIs10*) were established; both show the same phenotypes. *ynIs9* animals were crossed to *flp-1(yn2)* animals.
29. H. R. Horvitz, M. Chalfie, C. Trent, J. E. Sulston, P. D. Evans, *Science* **216**, 1012 (1982).
30. L. Ségalat, D. A. Elkes, J. M. Kaplan, *ibid.* **267**, 1648 (1995).
31. O. Chiba, K. Sasake, H. Higuchi, K. Takashima, *Neurosci. Res.* **15**, 255 (1992); K. Payza and H.-Y. T. Yang, *J. Neurochem.* **60**, 1894 (1993); G. J. Chin, K. Payza, D. A. Price, M. J. Greenberg, K. E. Doble, *Biol. Bull.* **187**, 185 (1994).
32. E. Linguegila, G. Champigny, M. Lazdunski, P. Barbry, *Nature* **378**, 730 (1995).
33. J. E. Mendel *et al.*, *Science* **267**, 1652 (1995); L. Brundage *et al.*, *Neuron* **16**, 999 (1996); R. R. Zwaal *et al.*, *Cell* **86**, 619 (1996).
34. L. Brundage, W. Chen, P. Sternberg, personal communication.
35. We thank R. H. A. Plasterk for generously screening for and providing the *flp-1*::Tc1 insertional strain NL242 *(pk41)*; L. Brundage, J. Mendel, P. Sternberg, J. Kaplan, L. Avery, and R. Korswagen for providing G protein–subunit mutants, advice on assays, and communication of unpublished results; H. R. Horvitz for providing mapping strains; A. Fire for providing microinjection vectors; J. Cherry and E. Widmaier for patiently providing help with the statistical analyses; S. Craven, H. Field, G. Jang, Y. Honzano, and C. Milliken for graciously providing technical assistance; T. Gilmore for comments on the manuscript; and members of the lab for helpful discussions. Supported in part by grants from NSF (IBN9320262) and NIH (AG00708) to C.L.

23 March 1998; accepted 5 August 1998

Prevention of Cardiac Hypertrophy in Mice by Calcineurin Inhibition

Mark A. Sussman, Hae W. Lim, Natalie Gude, Tyler Taigen, Eric N. Olson, Jeffrey Robbins, Melissa C. Colbert, Antonio Gualberto, David F. Wieczorek, Jeffery D. Molkentin*

Hypertrophic cardiomyopathy (HCM) is an inherited form of heart disease that affects 1 in 500 individuals. Here it is shown that calcineurin, a calcium-regulated phosphatase, plays a critical role in the pathogenesis of HCM. Administration of the calcineurin inhibitors cyclosporin and FK506 prevented disease in mice that were genetically predisposed to develop HCM as a result of aberrant expression of tropomodulin, myosin light chain–2, or fetal β-tropomyosin in the heart. Cyclosporin had a similar effect in a rat model of pressure-overload hypertrophy. These results suggest that calcineurin inhibitors merit investigation as potential therapeutics for certain forms of human heart disease.

Heart failure is the major cause of disability and morbidity in the United States and affects about 700,000 individuals each year (*1*). Heart disease can arise from extrinsic stimuli such as hypertension or from intrinsic defects within the heart itself. HCM is the most common form of intrinsic heart disease and has been cited as the most frequent cause of sudden death in young people (*1*). HCM is defined by a generalized enlargement of the myocardium, but it can progress to heart dilation, functional insufficiency, and failure (*1*). Several intrinsic cardiomyopathies are caused by genetic mutations in contractile proteins that organize into repetitive units known as sarcomeres. Mutations have been identified in the genes encoding β-myosin heavy chain (MHC), cardiac troponin T, α-tropomyosin, myosin-binding protein C, myosin light chains (MLC), and cardiac α-actin (*2*). Normal sarcomeric function is associated with a basal concentration of intracellular calcium, which regulates contractility. It has been postulated that mutations in sarcomeric proteins lead to increases in intracellular calcium in order to maintain contractility and cardiac output (*3*). However, increases in basal calcium concentrations are also associated with cardiac hypertrophy.

We have shown that calcineurin, a calcium-regulated phosphatase, initiates cardiac hypertrophy when it is expressed in a constitutively active form in the heart of transgenic mice (*4*), suggesting a link between calcium concentration and a calcium-regulated signaling molecule in the heart. Calcineurin is activated by prolonged increases in basal concentrations of calcium, but not by transient calcium spikes associated with the activation of calcium-calmodulin–dependent kinase II (CaMKII) and mitogen-activated protein kinase (MAPK) (*5*). Together, these data suggest that calcineurin may play a pivotal role in signaling maladaptive hypertrophy in response to alterations in calcium handling in the heart.

To test this hypothesis, we treated four transgenic mouse models of cardiomyopathy and a rat model of pressure-overload hypertrophy with the calcineurin inhibitors cyclosporin (CsA) and FK506. We initially tested a mouse model of dilated cardiomyopathy caused by cardiac-specific overexpression of

M. A. Sussman, H. W. Lim, N. Gude, T. Taigen, J. Robbins, M. C. Colbert, J. D. Molkentin, Division of Molecular Cardiovascular Biology, Children's Hospital Medical Center, 3333 Burnet Avenue, Cincinnati, OH 45229, USA. E. N. Olson, Department of Molecular Biology and Oncology, University of Texas Southwestern Medical Center, Dallas, TX 75235, USA. A. Gualberto, Department of Physiology and Biophysics, Case Western Reserve University School of Medicine, Cleveland, OH 44106, USA. D. F. Wieczorek, Department of Molecular Genetics, University of Cincinnati, Cincinnati, OH 45267, USA.

*To whom correspondence should be addressed. E-mail: molkj0@chmcc.org